ISSN 0031-918X, The Physics of Metals and Metallography, 2006, Vol. 101, Suppl. 1, pp. S6–S9. © Pleiades Publishing, Inc., 2006.

MAGNETIC MECHANISMS OF SUPERCONDUCTIVITY

Spin-Fluctuation and Spin–Exciton Mechanisms of Superconductivity in Cuprates[1]

M. M. Korshunov[a], S. G. Ovchinnikov[a], and A. V. Sherman[b]

[a] *Kirensky Institute of Physics, Siberian Division, Russian Academy of Sciences, Sibirskii trakt 10/7, Akademgorodok, Krasnoyarsk, 660036 Russia*

[b] *Institute of Physics, University of Tartu, Riia 142, 51014 Tartu, Estonia*

Abstract—The properties of the normal and superconductive phases of *p*- and *n*-type cuprates are investigated in terms of the appropriate low-energy models in the approximation beyond Hubbard I with inclusion of spin fluctuations. The comparison of the singlet–triplet *t–J* model with the *t–J* model shows that the spin–exciton mechanism originated from the singlet–triplet hybridization contributes only slightly to the phase diagram of the *p*-type systems.

PACS numbers: 74.20.Mn, 74.72.-h

DOI: 10.1134/S0031918X06130035

High-T_c superconducting cuprates (HTSCs) consist of two major classes: a *p*-type class, which stands for hole-doped cuprates ($La_{2-x}Sr_xCuO_4$ (LSCO), $Bi_2Sr_2CaCu_2O_{8+\delta}$ (Bi2212), $YBa_2Cu_3O_{7+\delta}$ (YBCO), etc.); and an *n*-type class, which includes electron-doped cuprates ($Nd_{2-x}Ce_xCuO_4$ (NCCO), $Pr_{2-x}Ce_xCuO_4$ (PCCO), etc.). Despite the similar crystal structure and the presence of the common base element—CuO_2 plane—in all HTSCs, the experimentally observed properties of these two classes are quite different (see, e.g., [1, 2]).

To properly describe strong electron correlations in cuprates, we have to start with an appropriate model and an appropriate set of parameters. As a starting model that adequately describes the electronic structure of the cuprates, it is convenient to use the three-band Emery *p–d* model or the multiband *p–d* model [3]. While the former is simpler, it does not contain some significant features such as copper d_{z^2} orbitals and p_z orbitals of the apical oxygens. The nonzero occupancy of d_{z^2} orbitals was revealed in XAS and EELS experiments, which give a 1.5–10% occupancy for d_{z^2} orbitals [4, 5] and a 15% doping-dependent occupancy for p_z orbitals [6] in all *p*-type HTSCs. In order to take into account these facts, the multiband *p–d* model was used to derive an effective low-energy model by excluding the intersubband hopping between low (LHB) and upper (UHB) Hubbard subbands via canonical transformations. The obtained effective Hamiltonian [7] is asymmetric for *n*- and *p*-type systems: for electron-doped systems, the usual *t–J** model (*t–J* model with three-center-interaction terms) takes place, while the effective singlet–triplet *t–J** model corresponds to *p*-type superconductors. The reason why this asymmetry arises is as follows. There are two low-lying two-hole states: the Zhang–Rice-type singlet $^1A_{1g}$ and the triplet state $^3B_{1g}$. In the three-band model, the triplet state lies above the singlet state by an energy $\Delta_{ST} = \varepsilon_T - \varepsilon_S \propto 2$ eV and is unimportant in the low excitation-energy limit. However, it is a model-dependent result, and in the multiband *p–d* model, Δ_{ST} decreased due to the Hund coupling of two holes in $d_{x^2-y^2}$ and d_{z^2} copper orbitals and due to the additional hopping t'_{pd} from the d_{z^2} copper orbital to the p_z orbital of the apical oxygen. For realistic values of the parameters in the multiband *p–d* model, $\Delta_{ST} \le 0.5$ eV [8, 9]. Thus, we conclude that we cannot drop out singlet–triplet mixing, and the complicated structure of the valence band near the binding energies ~0.5 eV in *p*-type cuprates is related to the triplet band and singlet–triplet hybridization. In the *n*-type system, there is no triplet state in the $d^{10}p^6$ configuration and the effective model is much simpler (*t–J** model). Both the *t–J** model and the effective singlet–triplet *t–J** model contain three-center interaction terms whose importance for the superconducting phase was shown in [10]. The model parameters are not free, since there is a strict relationship between the microscopic parameters and the effective model parameters [11, 12]. The microscopic parameters were determined in the framework of the generalized tight-binding method for undoped LSCO and NCCO and remain constant with doping. Since the dependence of the model parameters on distance is known from the explicit construction of Wannier states in the CuO_6 unit cell, the subsequent calculations are performed with inclusion of the hoppings and exchanges up to the fifth coordination shell. Since most experimental data show convincingly that the symmetry of the superconducting order

[1] The text was submitted by the authors in English.

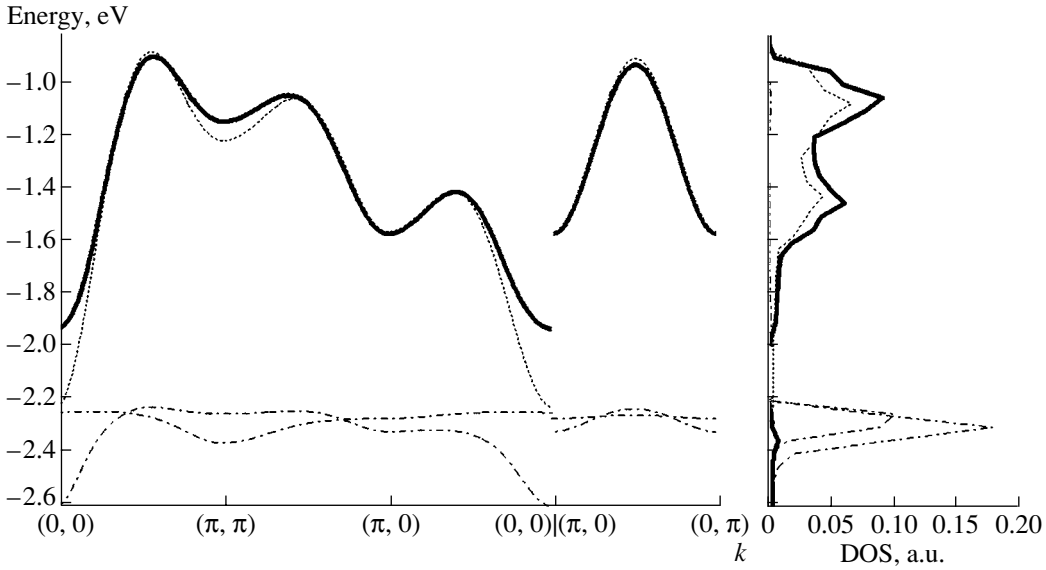

Fig. 1. Quasiparticle dispersion and partial density of states for *p*-type cuprates in the *t*–*J** model (dotted curve) and in the singlet–triplet *t*–*J** model (solid curve corresponds to the singlet subband, and the dot-and-dash curves correspond to two triplet subbands).

parameter is of the $d_{x^2-y^2}$ type, in this work we will consider only this pairing symmetry.

The effective models were investigated in the framework of the equation-of-motion method in the generalized Hartree–Fock approximation. To solve the equations obtained, we have used a decoupling procedure that includes the short-range magnetic order beyond the Hubbard-I approximation: $\langle X_f^{\sigma\sigma} X_g^{\sigma'\sigma'} \rangle \longrightarrow n_p^2 + \frac{\sigma}{\sigma'}\frac{1}{2} C_{fg}$ and $\langle X_j^{\sigma\bar{\sigma}} X_g^{\bar{\sigma}\sigma} \rangle \longrightarrow C_{fg}$. Here, n_p is the occupancy of the one-particle states, and $C_{f\sigma} = \langle X_f^{\sigma\bar{\sigma}} X_g^{\bar{\sigma}\sigma} \rangle = 2\langle S_f^z S_g^z \rangle$ are the spin-correlation functions.

In order to calculate spin-correlation functions $C_{f\sigma}$, the two-dimensional *t*–*J* model of the CuO_2 planes was used. The self-energy equations on Green's functions built with the Hubbard operators were obtained with the help of the Mori formalism that makes it possible to present these functions as continued fractions. The elements of these fractions for electron and spin Green's functions contain correlation functions for neighboring sites, while the other elements of the fractions are higher-order Green's functions. The latter can be approximated by decoupling with vertex corrections [13, 14]. The vertex corrections are determined from the zero-site magnetization restriction in the paramagnetic case under consideration. This condition in combination with the self-energy equations on electron and spin Green's functions, and the self-consistency conditions for the correlation functions form a closed set of equations that is solved iteratively for a fixed chemical potential and a fixed temperature. The results of the calculations with small clusters [15, 16] are in good agreement with exact diagonalization and quantum Monte Carlo studies. In this work, we calculated the spin correlation function in the above-described approach from the spin Green's function on a 20×20 grid.

A comparison of the *t*–*J** model with the effective singlet–triplet *t*–*J** model is illustrated in Fig. 1. A tendency that is general to both models can be seen: the interplay of spin fluctuations and three-center-interaction terms gives a tendency to restore antiferromagnetic (AFM) symmetry of the Brillouin zone—a local symmetry around $(\pi/2, \pi/2)$ and $(\pi, 0)$ points appears in the dispersion curve due to the development of a short-range order. This leads to the appearance of a saddle point near $(\pi, 0.4\pi)$ which gives an additional Van Hove singularity [17]. This singularity gives an additional "dome" of superconductivity at a low doping concentration with a maximum $T_c(x)$ at $x_{opt} \approx 0.15$ (see Fig. 2). The well-known "dome" of superconductivity at higher concentrations with $x_{opt} \approx 0.53$ is due to another Van Hove singularity corresponding to the saddle point at $(\pi, 0)$. These results can be qualitatively explained as follows. In the Bardeen–Cooper–Schrieffer theory, $T_c \propto \exp(-1/N(\varepsilon_F)V)$, where $N(\varepsilon_F)$ is the density of states at the Fermi level and V is the effective attraction. So, if there is a singularity in the density of states, then, upon doping, ε_F will reach this singularity, and there will be a maximum in $T_c(x)$.

In *p*-type systems, apart from the spin-fluctuation mechanism typical of the *t*–*J* model, there is an additional spin–exciton mechanism of pairing [18], and the phase diagram $T_c(x)$ for the effective singlet–triplet model is different from the phase diagram of the usual *t*–*J* model. Namely, in the nearest-neighbor approximation, neglecting three-center-interaction terms and spin fluctuations, the optimum doping level is changed from

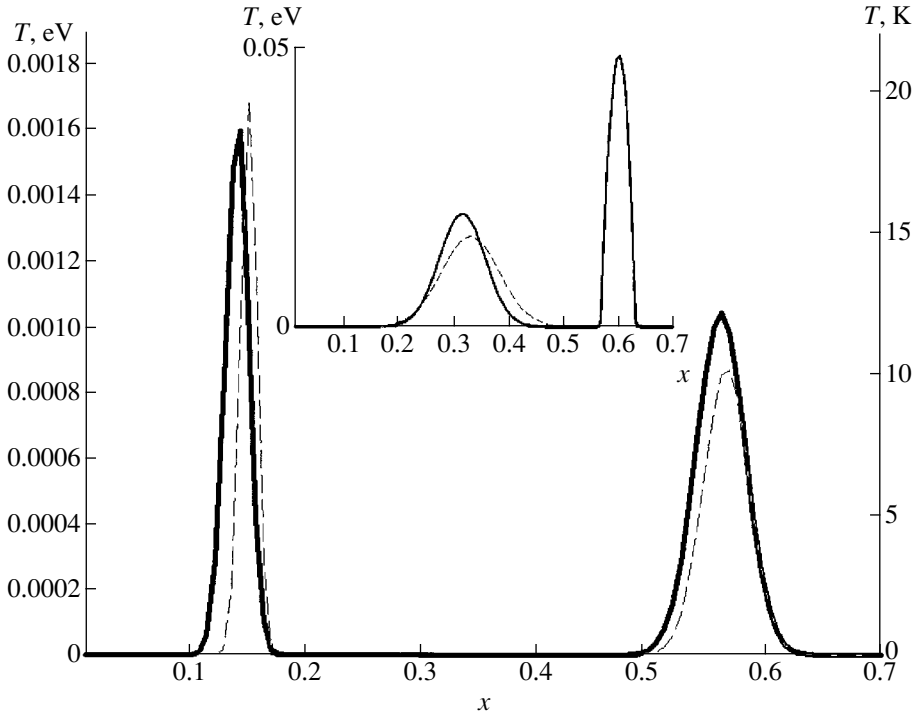

Fig. 2. Phase diagram of *p*-type cuprates: the $T_c(x)$ dependence calculated in the *t*–*J** model (dashed curve) and in the singlet–triplet *t*–*J** model (solid curve) are shown. The inset demonstrates the calculated $T_c(x)$ dependence for both these models in the nearest-neighbor approximation without three-center-interaction terms and without spin fluctuations.

$x = 0.33$ typical of the *t*–*J* model to $x = 0.315$, and the maximum value of $T_c(x)$ increases as well. Also, a new "dome" of superconductivity appears around $x = 0.6$ due to a triplet subband (see inset in Fig. 2). However, taking into account the three-center terms, the spin fluctuations beyond the Hubbard I decoupling, and the hoppings and exchanges up to the fifth coordination shell, the influence of the singlet–triplet-induced superconducting pairing becomes small, as is seen from Fig. 2. The "dome" of superconductivity connected with the triplet subband shifts to higher doping concentrations ($x > 0.8$) and does not reveal itself in experiment.

In conclusion, we can say that we used the approximation that includes spin fluctuations beyond the Hubbard I approximation to investigate the superconducting phase with a $d_{x^2-y^2}$-gap symmetry in the effective low-energy model for cuprates. For the *p*-type cuprates, the influence of the singlet–triplet hybridization is analyzed. First, due to this hybridization, the spin–exciton mechanism of superconducting pairing takes place. A comparison with the *t*–*J** model shows that the spin–exciton mechanism leads to a small contribution to the phase diagram: the optimum-doping level becomes slightly lower and the maximum T_c becomes slightly higher. The smallness of this contribution is directly connected with the smallness of the hybridization matrix element between the singlet and triplet subbands. Also, an additional "dome" of superconductivity appears due to the triplet subband. However, this "dome" is located at too-high doping concentrations and can be neglected. In the *p*-type cuprates, our approach and approximations give only qualitative agreement with the experimental picture: our theory properly predicts only the value of optimum doping $x_{opt} \approx 0.15$, but the value of $T_c(x_{opt}) = 20$ K and the width of the superconducting "dome" is half as those observed experimentally. The distance between the chemical potential at optimum doping and the Van Hove singularity corresponding to a flat dispersion around $(\pi, 0)$ in our approach is equal to 0.52 eV, while in experiment it is less than 0.03 eV in all *p*-type systems [19]. We suppose that the main mechanism of superconductivity is the spin-fluctuation exchange, but in order to explain the complicated phase diagram of *p*-type HTSCs, one have to take into account other features of these compounds. Namely, the electron–phonon interaction and the magnetic frustrations, which take place in underdoped region and lead to a nonuniform magnetic state, the incommensurability of spin fluctuations, and the phase separation observed in *p*-type cuprates.

ACKNOWLEDGMENTS

We are grateful to V.V. Val'kov and D.M. Dzebisashvili for the stimulating discussion. This work was supported by the Russian Foundation for Basic Research (grant no. 03-02-16124); Russian Academy

of Sciences, Quantum Macrophysics Program; INTAS (grant no. 01-0654); ETF (grant no. 5548); Siberian Division of the Russian Academy of Sciences (Lavrent'ev Contest for Young Scientists); the Dynasty Foundation; and ICFPM.

REFERENCES

1. G. M. Luke et al., Phys. Rev. B: Condens. Matter **42**, 7981 (1990).
2. J. L. Peng et al., Phys. Rev. B: Condens. Matter **55**, R6145 (1997).
3. Yu. B. Gaididei and V. M. Loktev, Phys. Status Solidi B **147**, 307 (1988).
4. A. Bianconi et al., Phys. Rev. B: Condens. Matter **38**, 7196 (1988).
5. H. Romberg et al., Phys. Rev. B: Condens. Matter **41**, 2609 (1990).
6. C. H. Chen et al., Phys. Rev. Lett. **68**, 2543 (1992).
7. M. Korshunov and S. Ovchinnikov, Fiz. Tverd. Tela (St.-Petersburg) **43**, 399 (2001) [Phys. Solid. State **43**, 416 (2001)].
8. H. Kamimura and M. Eto, J. Phys. Soc. Jpn. **59**, 3053 (1990).
9. V. A. Gavrichkov et al., Zh. Eksp. Teor. Fiz. **118**, 422 (2000) [JETP **91**, 369 (2000)].
10. V. V. Val'kov et al., Pis'ma Zh. Eksp. Teor. Fiz. **75**, 450 (2002) [JETP Lett. **75**, 378 (2002)].
11. M. M. Korshunov et al., Physica C **402**, 365 (2004).
12. M. M. Korshunov et al., Zh. Eksp. Teor. Fiz. **126**, 642 (2004) [JETP **99**, 559 (2004)].
13. A. F. Barabanov and V. M. Berezovskii, Zh. Eksp. Teor. Fiz. **106**, 1156 (1994).
14. J. Kondo and K. Jamaji, Prog. Theor. Phys. **47**, 807 (1972).
15. A. Sherman and M. Schreiber, Phys. Rev. B: Condens. Matter Mater. Phys. **65**, 134520 (2002).
16. A. Sherman and M. Schreiber, Eur. Phys. J. B **32**, 203 (2003).
17. V. V. Val'kov and D. M. Dzebisashvily, submitted to JETP (2004).
18. S. G. Ovchinnikov, Pis'ma Zh. Eksp. Teor. Fiz. **64**, 23 (1996) [JETP Lett. **64**, 25 (1996)].
19. D. M. King et al., Phys. Rev. Lett. **70**, 3159 (1993).